Immune complex solubility and size govern individual Fc-gamma receptor responses: Novel biomarkers for autoimmune diseases

Haizhang Chen[1,2], Andrea Maul-Pavicic[3,4], Martin Holzer[5], Ulrich Salzer[3], Nina Chevalier[3], Reinhard E. Voll[3,4], Hartmut Hengel[1,2,*] & Philipp Kolb[1,2,*]

[1]Institute of Virology, University Medical Center, Albert-Ludwigs-University Freiburg, Hermann-Herder-Str. 11, 79104 Freiburg, Germany

[2]Faculty of Medicine, Albert-Ludwigs-University Freiburg, 79104 Freiburg, Germany

[3]Department of Rheumatology and Clinical Immunology, Medical Center - University of Freiburg, Faculty of Medicine, University of Freiburg, Hugstetterstr. 55, 79106 Freiburg, Germany

[4]Center for Chronic Immunodeficiency (CCI), Medical Center-University of Freiburg, Faculty of Medicine, University of Freiburg, Breisacherstr. 115, 79106 Freiburg, Germany

[5]Institute for Pharmaceutical Sciences, Albert-Ludwigs-University Freiburg, Hermann-Herder-Str. 9, 79104 Freiburg, Germany

*corresponding authors (Hartmut.hengel@uniklinik-freiburg.de)

One Sentence Summary: This study reveals selective activation of individual Fc-gamma receptors by soluble but not immobilized immune complexes, establishing a novel biomarker for autoimmune disease in humans and mouse models.

Abstract: Fc-gamma receptor (FcγR) activation by soluble IgG immune complexes (sICs) is thought to be a major mechanism of inflammation in certain autoimmune diseases such as systemic lupus erythematosus (SLE). A robust and scalable test system allowing for the detection and quantification of sIC bioactivity is missing. Therefore, we developed a comprehensive reporter cell panel capable of measuring the sIC-mediated activation of individual human and mouse FcγRs. We show that compared to human FcγRs IIB and III, human FcγRs I and IIA lack sensitivity to sICs. Further, the assay proved to be sensitive to sIC stoichiometry and size enabling us to demonstrate for the first time a complete translation of the Heidelberger-Kendall precipitation curve to FcγR responsiveness. This was validated using primary immune cells. The approach was applied to quantify sIC-mediated FcγR activation using sera from SLE patients or from mouse models of lupus and arthritis. Thus, in clinical practice, it might be employed as a test matrix toolbox enabling the evaluation of FcγR activation by sICs as a biomarker for disease activity in immune-complex mediated diseases.

Introduction

Immunoglobulin G (IgG) is the dominant immunoglobulin isotype in chronic infections and in antibody-mediated autoimmune diseases. The multi-faced effects of the IgG molecule rely both on the F(ab) regions, which recognize a specific antigen to form immune complexes (ICs), and the constant Fc region (Fcγ), which is detected by Fcγ receptors (FcγRs) found on most cells of the immune system (*1*). When IgG binds to its antigen ICs are formed, which, depending on the respective antigen, are either cell-bound or soluble (sICs). The composition of sICs is dependent on the number of epitopes recognized by IgG on a single antigen molecule and the ability of the antigen to form multimers. Fcγ-FcγR binding is necessary but not sufficient to activate FcγRs since physical receptor cross-linking generally underlies receptor activation (*2-5*). Firmly fixed cell bound ICs are readily able to cross-link FcγRs (*4,*

50 *6*). This condition induces various signaling pathways (*7-9*) which in turn regulate immune
51 cell effector functions (*10, 11*). It is also suggested that sICs can dynamically tune FcγR
52 triggering, implying that changes in sIC size directly impact FcγR responses (*6*). However,
53 the molecular requirements are largely unknown. Also, a functional reproduction of the
54 paradigmatic Heidelberger-Kendall precipitation curve, describing that the molecular size of
55 sICs determined by the antibody:antigen ratio dynamically tunes FcγR activation on and off
56 (*12, 13*), is so far missing.
57 In contrast to FcγR binding of monomeric ligands without consequences, IC-mediated FcγR
58 cross-linking initiates the full signal cascade followed by immune cell activation or inhibition,
59 resp. (*5, 8, 14, 15*). Human FcγRs are membrane resident receptors recognizing Fcγ. Among
60 all type I FcγRs, FcγRIIB (CD32B) is the only inhibitory one signaling via immunoreceptor
61 tyrosine-based inhibitory motifs (ITIMs) while the activating receptors are associated with
62 immunoreceptor tyrosine-based activation motifs (ITAMs). Another exception is FcγRIIIB
63 (CD16B), which is glycosylphosphatidylinositol (GPI)-anchored (*16-19*). FcγRI (CD64) is the
64 only receptor with high affinity binding to monomeric IgG not associated with antigen and is
65 primarily tasked with phagocytosis linked to antigen processing and pathogen clearance (*20,*
66 *21*). All the other FcγRs only efficiently bind to complexed, meaning antigen-bound IgG (*1,*
67 *16, 17*). While FcγRI, FcγRIIB and FcγRIIIA are able to recognize sICs, this has not been
68 reported for FcγRIIA (CD32A), rather this receptor has recently been shown to depend on the
69 neonatal Fc receptor (FcRn) or FcγRIIIB (CD16B) to do so (*22, 23*). Activation of FcγRs
70 leads to a variety of cellular effector functions such as antibody-dependent cellular
71 cytotoxicity (ADCC) by natural killer (NK) cells via FcγRIIIA, antibody-dependent cellular
72 phagocytosis (ADCP) by macrophages via FcγRI, cytokine and chemokine secretion by NK
73 cells and macrophages via FcγRIIIA. Further effector responses are reactive oxygen species
74 (ROS) production of neutrophils and neutrophil extracellular traps formation (NETosis) via
75 FcγRIIIB, dendritic cell (DC) maturation and antigen presentation via FcγRIIA and B cell

76 selection and differentiation via FcγRIIB (*10, 24-30*). Consequently, FcγRs connect and
77 regulate both innate and adaptive branches of the immune system. Various factors have been
78 indicated to influence the IC-dependent FcγR activation profiles, including Fcγ-FcγR binding
79 affinity and avidity (*31*), IgG subclass, glycosylation patterns and genetic polymorphism (*4,*
80 *24, 25, 32*), stoichiometry of antigen-antibody-ratio (*6, 30, 33*) and FcγR clustering patterns
81 (*34*). Specifically, Asn297-linked glycosylation patterns of the IgG Fc domain initiate either
82 pro- or anti-inflammatory effector pathways by tuning the binding affinity to activating versus
83 inhibitory FcγRs, respectively (*35*). However, despite being explored in proof-of-concept
84 studies, the functional consequences of these ligand features on a specific receptor are still not
85 fully understood. Therefore, an assay platform allowing for the systematic functional
86 assessment of IC-mediated FcγR activation is strongly required. While a previously
87 developed cell-based assay addresses sIC-mediated activation of the inhibitory FcγRIIB (*36*),
88 a platform allowing for the comprehensive analysis of all FcγRs is missing.
89 sICs and immobilized ICs represent different stimuli for the immune system (*22, 29*). Soluble
90 circulating ICs are commonly associated with certain chronic viral or bacterial infections (*37,*
91 *38*) and autoimmune diseases, such as systemic lupus erythematosus (SLE) or rheumatoid
92 arthritis (RA) (*39-41*). When accumulating and deposited in tissues sICs can cause local
93 damage due to inflammatory responses, classified as type III hypersensitivity (*42*). Typically,
94 sICs related disorders are characterized by systemic cytokine secretion which can be followed
95 by immune cell exhaustion and senescence (*43, 44*). In order to study sIC-dependent
96 activation of FcγRs in detail, we employed a cell-based assay which has been previously
97 utilized to study immobilized ICs (*45*) and adapted it into a sIC sensitive reporter system
98 capable of distinguishing the activation of individual FcγRs and their responses to varying
99 complex size. This approach allowed for the first time a complete reproduction of the
100 Heidelberger-Kendall precipitation curve measuring actual FcγR triggering. The assay
101 enables a quantification of clinically relevant sICs in sera from SLE patients and autoimmune-

102 prone mice with immune-complex-mediated arthritis and lupus using reporter cells expressing
103 chimeric mouse FcγRs.
104
105 **Results**
106 *Experimental assay setup*
107 The assay used in this study was adapted from a previously described cell-based FcγR
108 activation assay designed to measure receptor activation in response to opsonized virus
109 infected cells (*45*) or therapeutic Fc-fusion proteins (*46*). We complemented the assay setup to
110 enable measurement of sICs when incubated with reporter cells stably expressing the
111 ectodomains of the human FcγR fused to the signaling module of the mouse CD3-ζ chain
112 (FcγRI: Acc# LT744984; FcγRIIA(R): Acc# M28697; FcγRIIB/C: Acc# LT737639;
113 FcγRIIIA/B(V): Acc# LT737365). Ectodomains of FcγRIIIA and FcγRIIIB as well as
114 ectodomains of FcγRIIB and FcγRIIC are identical. Second generation reporter cells were
115 generated to improve stable expression of chimeric FcγRs compared to the transfectants used
116 in the original assay (*45*). To this end, BW5147 cells were transduced as described previously
117 via lentiviral transduction (*45, 47*). Human FcγR expression on transduced cells after
118 puromycin selection is shown in Fig. 1A. FcγR triggering is translated into activation of the
119 reporter cells and measured by quantification of endogenous IL-2 (mIL-2) secretion into the
120 cell culture supernatant using an anti-IL-2 sandwich ELISA as described previously (*45*). In
121 order to employ the original assay, designed to detect ICs on adherent virus-infected cells, for
122 the detection of soluble ICs we first determined the suspension of IgG achieved by pre-
123 incubating a 96 well ELISA microtiter plate with PBS/FCS blocking buffer. To this end, we
124 compared graded concentrations of FCS in the blocking reagent and measured the threshold at
125 which IgG (rituximab, Rtx) was no longer adsorbed to the plate and stayed abundantly in
126 solution. Fig. 1B demonstrates that FCS supplementation to 1% (v/v) or higher is sufficient to
127 keep IgG antibodies in solution and prevents binding to the plastic surface. Using this adapted

128 protocol, the assay now allowed for the sensitive detection and characterization of FcγR
129 interaction with immobilized ICs versus sICs as shown schematically in Fig. 1C. First, we set
130 out to test if monomeric IgG upon immobilization becomes an operational surrogate for IgG-
131 opsonized cells or immobilized ICs with regard to FcγR activation as suggested before (*48*).
132 As depicted in Fig. 2, there was no qualitative difference in FcγR activation between
133 immobilized Rtx, immobilized ICs (Rtx + rec. CD20) or Rtx-opsonized 293T-CD20 cells,
134 showing that FcγR cross-linking by clustered IgG alone is sufficient for receptor cross-linking
135 and activation. In contrast, sICs formed by monomeric CD20 peptide (aa 141-188) and Rtx
136 failed to activate FcγRs even at very high ligand concentrations. Based on this finding we
137 hypothesized that, in order to generate sICs able to activate FcγRs, antigens have to be
138 multivalent to achieve cross-linking of FcγRs. Of note, to reliably and accurately differentiate
139 between soluble and immobilized triggers using this assay, reagents for the generation of ICs
140 need to be of very high purity and consistent stability. Indeed, only combinations of
141 pharmaceutical therapy grade, i.e. ultra-pure mAbs and pure antigens (purified via size
142 exclusion chromatography) showed reproducible, dose-dependent and specific activation in
143 the reporter assay (data not shown).
144
145 *Quantification of human FcγR responsiveness to multimeric sICs*
146 To date, there are only few commercially available human IgG-antigen pairs that meet both
147 the above mentioned high grade purity requirements while also providing a multimeric
148 antigen. In order to meet these stipulations of ultra-pure synthetic soluble immune complexes
149 we focused on three pairs of multivalent antigens and their respective mAbs that were
150 available in required amounts enabling large-scale titration experiments; trimeric
151 rhTNFα:IgG1 infliximab (TNFα:Ifx), dimeric rhVEGFA: IgG1 bevacizumab (VEGFA/Bvz)
152 and dimeric rhIL-5: IgG1 mepolizumab (IL-5/Mpz). As lymphocytes express TNFα-receptors
153 I and II while not expressing receptors for IL-5 or VEGFA, we tested whether the mouse

154 lymphocyte derived BW5147 thymoma reporter cell line is sensitive to high concentrations of
155 rhTNFα. Toxicity testing revealed that even high concentrations up to 76.75 nM rhTNFα did
156 not affect viability of reporter cells (Fig. S1). Next, we measured the dose-dependent
157 activation of human FcγRs comparing immobilized IgG to soluble ICs using the FcγR
158 reporter cell panel (Fig. 3). Soluble antigen or mAb alone served as negative controls showing
159 no background activation even at high concentrations. Immobilized rituximab served as a
160 positive control for inter-experimental reference. We observed that all FcγRs are strongly
161 activated in a dose-dependent manner when incubated with immobilized IgG. Incubating the
162 FcγR reporter cells with sICs at identical molarities showed FcγRIIB/C and FcγRIIIA/B to be
163 efficiently activated by sICs, while in contrast, FcγRIIA and FcγRI did not respond to sICs.
164 We furthermore observed FcγRIIIA/B to be efficiently activated by sICs with responses even
165 surpassing those achieved with immobilized IgG for TNFα/Ifx and IL-5/Mpz ICs. FcγRIIB/C
166 showed a generally weaker reactivity towards sICs compared to immobilized ICs, especially
167 at high concentrations whereas an inversion of this order was seen for TNFα/Ifx and
168 VEGFA/Bvz ICs at lower concentrations. IL-5/Mpz, FcγRIIB/C and FcγRIIIA/B showed
169 similar responsiveness towards immobilized or sICs with a generally stronger activation on
170 immobilized ICs. These findings demonstrate that sICs of different composition vary in the
171 resulting FcγR activation pattern, most likely due to the antigens being either dimeric, trimeric
172 or different in size. As we observed differences in responses to sICs vs. immobilized ICs for
173 individual FcγR-ζ reporter cells, this indicates that FcγR ectodomains alone are already able
174 to differentiate between these triggers. To validate this observation in principle, we
175 determined FcγRIIIA activation using primary human NK cells isolated from PBMCs of
176 healthy donors. NK cells were chosen as they mostly express only one type of FcγR similar to
177 our reporter system. Measuring a panel of activation markers and cytokine responses by flow
178 cytometry, we observed a differential activation pattern depending on ICs being soluble or
179 immobilized at equal molarity (Fig. 4A). We chose IL-5/Mpz sICs as NK cells do not express

180 the IL-5 receptor. While MIP1-β responses were comparable between the two triggers,
181 degranulation (CD107a) and TNFα responses showed a trend towards lower activation by
182 sICs compared to immobilized IgG (Mpz). Strikingly, IFNγ responses were significantly
183 weaker when NK cells were incubated with sICs compared to immobilized IgG. In order to
184 confirm this hierarchy of responses and to enhance the overall low activation by Fcγ
185 compared to the PMA control, we changed the IC setup by generating reverse-orientation
186 sICs consisting of human FcγR-specific mouse mAbs and goat-anti-mouse IgG $F(ab)_2$
187 fragments. NK cell activation by reverse sICs was compared to NK cell activation by
188 immobilized FcγR specific mAbs (Fig. 4B). Here, we not only confirm our previous
189 observations regarding MIP-1β and IFNγ, but we also confirm significantly lower TNFα and
190 CD107a responses towards soluble complexes compared to immobilized mAbs. Importantly,
191 these experiments validate that sICs readily activate primary NK cells and induce
192 immunological effector functions. As in roughly 10% of the population NK cells express
193 FcγRIIC (*49-52*), we also tested if this receptor plays a role in our measurements. Using the
194 same three donors and an FcγRII specific mAb as described above, we did not observe an
195 FcγRII-mediated response. Accordingly, we conclude that FcγRIIC expression did not play a
196 role in our experiments (Fig. 4C). Taken together, we show that multivalent but not dimeric
197 soluble immune complexes govern primary NK cell response and FcγRIIIA/B activation (Fig.
198 2A).
199
200 *Measurement of FcγR activation in response to changing sIC size*
201 We observed that the dimeric sIC CD20:Rtx molecule complex completely failed to trigger
202 FcγRs, while potentially larger sICs based on multimeric antigens showed an efficient dose-
203 dependent FcγR activation. In order to determine whether BW5147 FcγR-ζ reporter cells are
204 able to respond to changes in sIC size, we tested cross-titrated amounts of antibody (mAb,
205 infliximab, Ifx) and antigen (Ag, rhTNFα). To this end, the reporter cells were incubated with

206 sIC of different mAb:Ag ratios by fixing one parameter and titrating the other. According to
207 the Heidelberger-Kendall precipitation curve (*12*) describing sIC size as being dependent on
208 the mAb:Ag ratio, this should result in varying sIC sizes as an excess of either antigen or
209 antibody results in the formation of smaller complexes compared to the large molecular
210 complexes formed at around equal molarity. Changes in sIC size due to a varying mAb:Ag
211 ratio were quantified using asymmetrical flow-field flow fractionation (AF4) (Fig. 5A and
212 Table S1). Fig. S2 shows a complete run of such an analysis. AF4 analysis identifies the
213 highest sIC mean molecular being approximately 2130 kDa at a 1:3 ratio (mAb Ifx : Ag TNF-
214 α) with sICs getting smaller with increasing excess of either antigen or antibody,
215 recapitulating a Heidelberger-Kendall-like curve. Incubation of the FcγR reporter cells with
216 ICs of varying size indeed shows that the assay is sensitive to exactly monitor changes in sIC
217 size (Fig. 5B). Accordingly, both FcγR types showed the strongest responses at mAb:Ag
218 ratios of approximately 1:3. We then set out to test the accuracy of our reporter cell assay as a
219 surrogate for primary human immune cells expressing FcγRs. To this end, we tested primary
220 NK cells from three individual donors and measured NK cell MIP1-β upregulation in
221 response to synthetic sICs of varying size and composition again using a similar assay setup
222 optimized for NK cell activation. We chose MIP-1β upregulation as a cell surface marker to
223 measure NK cell activation as it showed the highest responsiveness in previous experiments
224 (Fig. 4). We could observe that primary immune cells expressing FcγRIIIA respond to IC
225 size, confirming our assay to be an accurate surrogate for primary immune cell responses to
226 soluble ICs (Fig. 5C). Convincingly, NK cell responses to sICs generated from trimeric
227 antigen (rhTNFα) peaked at a different mAb:Ag ratio compared to NK cell responses to sICs
228 generated from dimeric antigens (rhIL-5 and rhVEGFA). Of note, TNFα and VEGFA activate
229 resting NK cells thus leading to higher MIP1-β positivity when NK cells are incubated in the
230 presence of excess antigen. As NK cells do not express IL-5 receptor, this effect is not
231 observed in the presence of excess IL-5. Regarding TNFα, NK cells still show a stronger

232 activation by sICs generated under optimal mAb:Ag ratios compared to conditions where
233 excess antigen is used. The data reveal a direct correlation between sIC size and effector
234 responses. Conversely, when changing antibody concentrations using fixed amounts of
235 antigen, a consistent reduction of NK cell activation is observed in the presence of excess IgG
236 for all three mAb/Ag pairs.
237
238 *Quantification of sIC bioactivity in sera of SLE patients*
239 In order to apply the assay to a clinically relevant condition associated with the occurrence of
240 sICs we measured circulating sICs present in the serum of SLE patients with variable disease
241 activity. Sera from 4 healthy donors and 25 SLE patients were investigated for FcγRIIIA/B
242 and FcγRIIB/C activation. Reporter cells readily produced IL-2 in response to patient sera in a
243 dose-dependent manner (shown exemplarily for some SLE patients, see Fig. 6A), which was
244 not the case when sera from healthy controls were tested. Consistent with the observation that
245 FcγRI and FcγRIIA do not respond to synthetic sICs, reporter cells expressing these receptors
246 did also not respond to the tested serum samples (Fig. 6A, lower panel). While this reaction
247 pattern already indicated that sICs are the reactive component measured in SLE patients' sera,
248 we further demonstrate that FcγRIIIA/B and FcγRIIB/C activation depends on the presence of
249 serum ICs by analyzing patient serum before and after polyethylene glycol (PEG)
250 precipitation and depletion of sICs (Fig. 6B). Next, we calculated the area under the curve
251 (AUC) values for all 25 SLE patient titrations and normalized them to the AUC values
252 measured for healthy individuals. The resulting index values were then correlated with
253 established biomarkers of SLE disease activity, such as anti-dsDNA titers (α-dsDNA) and
254 concentrations of the complement cleavage product C3d (Fig. 6C). We observed a significant
255 correlation between our FcγRIIIA/B activation index values and both of the determined
256 disease activity markers, anti-dsDNA titers and C3d concentration ($p=0.0465$ and $p=0.0052$,
257 respectively). FcγRIIB/C on the other hand showed no significant correlation with either

258 biomarker. We assume these interrelations may be due to the influence of IgG sialyation
259 found to be reduced in active SLE (*53*). Generally, de-sialylation of IgG leads to stronger
260 binding by the activating receptors FcγRI, FcγRIIA and FcγRIII while it reduces the binding
261 affinity of the inhibitory FcγRIIB (*54*). In sum, our assay allows the indirect quantification of
262 clinically relevant sICs in sera of SLE patients.
263
264 *Assay application to clinically relevant in vivo lupus and arthritis mouse models*
265 BW5147 reporter cells stably expressing chimeric mouse as well as rhesus macaque FcγRs
266 have already been generated using the here described methodology and were successfully
267 used to measure FcγR activation by opsonized adherent cells in previous studies (*47, 55*)
268 (mFcγR reporter cells). As the human FcγR reporter cells described here are sensitive to
269 certain sICs, we next aimed to translate the assay to clinically relevant animal models. To this
270 end, we incubated previously described FcγR reporter cells expressing chimeric mouse FcγRs
271 (*47*) with sera from lupus (NZB/WF1) or arthritis (K/BxN) mice with active autoimmune
272 disease. The reporter assay was performed as described above. We chose to measure the
273 stimulation of the activating receptors, mFcγRIII and mFcγRIV, that correspond to human
274 FcγRIII and show a similar cellular distribution and immune function (*16*). Incubation with
275 synthetic sICs generated from rhTNFα and mouse-anti-hTNFα IgG1 showed both of the
276 mFcγR reporter cells to be equally responsive to sICs (Fig. 7A). Parental BW5147 cells
277 expressing no FcγRs served as a control. The sera of three mice per group were analysed and
278 compared to sera from wildtype C57BL/6 mice, which served as a healthy control. C57BL/6
279 mice were chosen, as healthy K/BxN or NZB/WF1 mice cannot be reliably defined. This is
280 due to the unpredictable disease progression in these mouse models starting from a young age.
281 We consistently detected mFcγR activation by sera from K/BxN or NZB/WF1 compared to
282 C57BL6 mice (Fig. 7B). While the mFcγRIII responses were generally high and similar
283 between K/BxN and NZB/WF1 mice, mFcγRIV responsiveness attended to be lower and

284 individually more variable. Altogether, the assay enables the reliable detection of sICs in sera
285 of mice with immune-complex mediated diseases making it a promising novel tool to monitor
286 sICs as a biomarker of disease activity.
287
288 **Discussion**
289 In this study we established, validated and applied a new assay system that is able for the first
290 time to selectively detect soluble multimeric immune complexes as discrete ligands of FcγR.
291 Major findings are i) that sICs cross-link and trigger human FcγRs IIB/C and IIIA/B but are
292 neglected by activating FcγRI and IIA; ii) that sICs potency is strictly stoichiometry- and size-
293 dependent and thus reproducing the classical Heidelberger-Kendall curve iii) that the overall
294 functional design of FcγRs is adapted to physical cross-linking by soluble vs. membrane-
295 bound immune complexes. The new test system has various obvious applications in medicine
296 and pharmacy.
297
298 *A novel assay for the quantification of disease-associated as well as synthetic sICs*
299 The new approach presents an important and implementable advancement in immunological
300 methodology as it enables the sensitive detection of receptor-activating ICs by a relatively
301 simple, scalable *in vitro* bioassay with high-throughput potential. Based on our pilot study
302 demonstrating that the sIC-mediated FcγRIII activation correlated with SLE disease markers,
303 this is of great value for larger prospective clinical studies in patients with autoimmune
304 diseases such as systemic lupus erythematosus (SLE) and rheumatoid arthritis (RA), where
305 circulating ICs have long been shown to crucially contribute to tissue damage and disease
306 manifestations (*40, 41, 56-58*). Disease-associated, endogenous sICs can also occur during
307 infection, e.g. generated after antibody-mediated destruction of pathogenic viruses or
308 microbes or probably more likely due to the oligomeric nature of numerous viral and bacterial
309 structural proteins generated e.g. by SARS-CoV2 (*59-61*) HIV and hepatitis B virus (HBV)

310 infection, during which circulating sICs are generated (*37, 62*). As the assay also enables the
311 sensitive and quantitative measurement of FcγR ligand bioactivity it allows the detection of
312 sICs not only in clinical specimens but also pharmaceutical preparations of IgG and Fc-fusion
313 proteins for therapeutic use (*46*). The presence of ICs in therapeutic preparations or sIC
314 formation following patient treatment is unwanted due to the risk of side effects such as
315 lupus-like syndrome which has been linked to mAb treatment in patients receiving infliximab
316 (*63*) or bevacizumab (*64*), both mAbs used in this study. As this assay is highly sensitive to
317 any aggregation of IgG, it also represents a tool to control the purity, quality and stability of
318 mAb preparations produced for therapeutic use in patients. In addition, the assessment of sIC-
319 mediated FcγR activation allows for optimization of mAbs and Fc-fusion proteins regarding
320 their molecular design and manufacturing. Specifically, Fc-molecules targeting cytokines and
321 soluble factors, which result in sIC formation, could be designed for reduced or enhanced
322 FcγR activation such as glyco-engineered mAbs or LALA-mutant mAbs (*65, 66*). Notably,
323 the scalability of this cell-based test system does allow for large-scale screening of samples.
324
325 *sICs form FcγR ligands with distinct functional profiles*
326 While immobilized ICs decorating infected cells, viral particles or microbial surfaces restrict
327 their triggering effect to a single immune cell residing in very close vicinity, sICs can rapidly
328 disseminate reaching a high number of immune effector cells thus developing a systemic
329 effect with far reaching and long-lasting or even threatening consequences for the host as a
330 whole. This could explain the very tight control of sIC governed effector programs and the
331 unresponsiveness of activating receptors like FcγRI and IIA. We also observed a difference in
332 the response patterns for FcγRIIIA/B and FcγRII/B/C depending on the solubility of clustered
333 IgG (immobilized versus soluble ICs) which we validated for FcγRIIIA using primary human
334 NK cells (Fig. 4 and 5C). Importantly,only multimeric but not dimeric sICs can trigger FcγR
335 activation. This highlights the fundamental structural influence of the particular antigen as

336 well as the IgG molecule on sIC dimension and subsequent FcγR-mediated signal processing.
337 The ability of the here described assay to define and quantify the activation of individual
338 FcγRs by sIC ligands is not achievable using primary immune cells due to redundant immune
339 responses upon FcγR activation and complex, overlapping expression pattern of FcγRs.
340 Finally, and in contrast to primary human cells, murine BW5147 reporter cells are largely
341 inert to human cytokines, which provides a key advantage to measure FcγR activation
342 selectively in human samples. Notably, the two basically sIC-responsive human FcγR types,
343 i.e. FcγRIIIA/B and FcγRIIB, are either highly activating versus strongly inhibitory and thus
344 show a mutually exclusive expression pattern (ref. review, z.B. Ravetch und Falk). FcγRIIIA
345 mediates ADCC elicited by NK cells and the induction of a pro-inflammatory cytokine profile
346 by $CD16^{+}$ monocytes, while FcγRIIIB is a GPI-anchored receptor on neutrophils. FcγRIIB is
347 an inhibitory receptor expressed by B cells and dendritic cells (DCs) regulating B cell
348 activation, antibody production by plasma cells and the activation state of DCs, while the
349 activating FcγRIIC is found on NK cells mediating ADCC. However, as FcγRIIC is only
350 expressed by roughly 10% of the human population, its role is still poorly understood (*49-52*).
351 Given the here shown fundamental difference in FcγR reactivity towards multimeric sICs
352 versus immobilized IgG it is tempting to speculate that FcγRIIIA/B- and FcγRIIB/C-positive
353 immune cells might have evolved to differentially perceive these different FcγR ligands (sICs
354 versus membrane bound insoluble ICs) and translate them into distinct reaction patterns. This
355 could be achieved by differences in receptor density, signal transduction or regulation of
356 receptor expression. Consulting the literature indeed supports our hypothesis with neutrophils,
357 B cells and NK cells being efficiently activated by sICs via essentially identical receptor
358 ectodomains (*18, 28, 67, 68*), while the immunological outcome of their triggering very much
359 differs.
360
361

362 *Dynamic sIC size measurement and monitoring of bioactivity in sIC-associated diseases*

363 We provide for the first time a simultaneous functional and biophysical assessment of the
364 paradigmatic Heidelberger-Kendall precipitation curve (*12, 13*). While previous work already
365 revealed that large and small sICs differentially impacts IL-6 production in PBMCs (*6*), the
366 dynamics of FcγR activation resulting from constant changes in sIC size have not been
367 explored on a systematic basis. This was undertaken in this study by directly analyzing
368 synthetic ICsformed by highly pure recombinant components via AF4 (Fig. 5A, Fig. S2,
369 Table S1). Our data document that sIC size is indeed governed by antibody:antigen ratios
370 covering a wide range of sizes up to several megadaltons. In the presence of increasing
371 amounts of antibody or antigen deviating from an optimal antibody:ratio, sIC size steadily
372 decreases. Further, by the measurement of FcγR activation we now translate sIC size directly
373 to asimple but precise read-out. In doing so, we show that sIC size essentially tunes FcγR
374 activation on and off. Thus, our new test system can not only contribute to the functional
375 detection and quantification of clinically relevant sICs but also provides a starting point on
376 how to avoid pathological consequences by influencing the sIC size, for example by
377 administering therapeutic antibodies or recombinant antigens in optimized concentrations,
378 thus becoming relevant in clinical pharmacokinetics.

379

380 *Limitations of the reporter system and conclusions*

381 While it is known that FcγRIIA requires FcγRIIIB or FcRn to efficiently respond to ICs (*22,*
382 *23, 69*), unexpectedly, we found that FcγRI is not activated by sICs in our assay. We assume
383 that FcγRI interaction with sICs might require a native cellular environment given that a
384 major function of this FcγR is the uptake and processing of antigen via ICs even in the
385 absence of a signaling motif (*21*). However, we find that FcγRI ectodomains alone are not
386 responsive to sICs implying a thoroughly different cross-linking threshold for FcγRI
387 compared with FcγRIIB and IIIA/B. This feature is possibly linked to its molecular

388 architecture being the only high-affinity FcγR with three extracellular Ig domains compared
389 to the two domains found in other FcγRs with lower affinity to monomeric IgG. This
390 observation also reflects a general consideration regarding the BW5147 reporter system.
391 While providing a robust and uniform read-out using a scalable cell-based approach, the assay
392 is not able to reflect native immune cell functions governed by cell-intrinsic signalling
393 cascades. The major advancements of this reporter system include i) a higher accuracy
394 regarding FcγR activation compared to merely affinity measurements, ii) an sIC size
395 dependent quantification of FcγR responsiveness and iii) the identification of FcγR activating
396 sICs in autoimmunity and infection. Finally, this scalable, sensitive and robust system to
397 detect FcγR activating sICs in clinical samples might enable their identification in diseases
398 that have not been linked to sIC-mediated pathology, yet.
399
400 **Materials and Methods**
401
402 *Cell culture:* All cells were cultured in a 5% CO_2 atmosphere at 37°C. BW5147 mouse
403 thymoma cells (BW, obtained from ATCC: TIB-47) were maintained at $3x10^5$ to $9x10^5$
404 cells/ml in Roswell Park Memorial Institute medium (RPMI GlutaMAX, Gibco)
405 supplemented with 10% (vol/vol) fetal calf serum (FCS, Biochrom), sodium pyruvate (1x,
406 Gibco) and β-mercaptoethanol (0.1 mM, Gibco). 293T-CD20 (kindly provided by Irvin Chen,
407 UCLA (*70*)) were maintained in Dulbecco's modified Eagle's medium (DMEM, Gibco)
408 supplemented with 10% (vol/vol) FCS.
409
410 *FcγR receptor activation assay:* FcγR activation was measured adapting a previously
411 described cell-based assay (*45, 71*). The assay was modified to measure FcγR activation in
412 solution. Briefly, $2x10^5$ mouse BW-FcγR (BW5147) reporter cells were incubated with
413 synthetic sICs or diluted serum in a total volume of 100 µl for 16 h at 37°C and 5% CO_2.

414 Incubation was performed in a 96-well ELISA plate (Nunc maxisorp) pre-treated with
415 PBS/10% FCS (v/v) for 1 h at 4°C. Immobilized IgG was incubated in PBS on the plates prior
416 to PBS/10% FCS treatment. Reporter cell mIL-2 secretion was quantified via ELISA as
417 described (*45*).
418
419 *Recombinant antigens and monoclonal antibodies to form sICs:* Recombinant human (rh)
420 cytokines TNF, IL-5, and VEGFA were obtained from Stem Cell technologies. Recombinant
421 CD20 was obtained as a peptide (aa141-188) containing the binding region of rituximab
422 (Creative Biolabs). FcγR-specific mAbs were obtained from Stem Cell technologies (CD16:
423 clone 3G8; CD32: IV.3). Reverse sICs were generated from these receptor-specific antibodies
424 using goat-anti-mouse IgG $F(ab)_2$ fragments (Invitrogen) in a 1:1 ratio. Pharmaceutically
425 produced humanized monoclonal IgG1 antibodies infliximab (Ifx), bevacizumab (Bvz),
426 mepolizumab (Mpz) and rituximab (Rtx) were obtained from the University Hospital
427 Pharmacy Freiburg. Mouse anti-hTNFα (IgG2b, R&D Systems, 983003) was used to generate
428 sICs reactive with mouse FcγRs. sICs were generated by incubation of antigens and
429 antibodies in reporter cell medium or PBS for 2 h at 37°C.
430
431 *Lentiviral transduction:* Lentiviral transduction of BW5147 cells was performed as described
432 previously (*47, 55*). In brief, chimeric FcγR-CD3ζ constructs (*45*) were cloned into a
433 pUC2CL6IPwo plasmid backbone. For every construct, one 10-cm dish of packaging cell line
434 at roughly 70% density was transfected with the target construct and two supplementing
435 vectors providing the VSV gag/pol and VSV-G-env proteins (6 µg of DNA each) using
436 polyethylenimine (22.5 µg/ml, Sigma) and Polybrene (4 µg/ml; Merck Millipore) in a total
437 volume of 7 ml (2 ml of a 15-min-preincubated transfection mix in serum-free DMEM added
438 to 5 ml of fresh full DMEM). After a medium change, virus supernatant harvested from the
439 packaging cell line 2 days after transfection was then incubated with target BW cells

440 overnight (3.5 ml of supernatant on 10^6 target cells), followed by expansion and pool
441 selection using complete medium supplemented with 2 µg/ml of puromycin (Sigma) over a
442 one week culture period.
443
444 *BW5147 toxicity test:* Cell counting was performed using a Countess II (Life Technologies)
445 according to supplier instructions. Cell toxicity was measured as a ratio between live and dead
446 cells judged by trypan blue staining over a 16 h time frame in a 96well format (100 µl volume
447 per well). BW5147 cells were mixed 1:1 with Trypan blue (Invitrogen) and analysed using a
448 Countess II. rhTNFα was diluted in complete medium.
449
450 *human IgG suspension ELISA:* 1 µg of IgG1 (rituximab in PBS, 50 µl/well) per well was
451 incubated on a 96well microtiter plate (NUNC Maxisorp) pre-treated (2h at RT) with PBS
452 supplemented with varying percentages (v/v) of FCS (PAN Biotech). IgG1 bound to the
453 plates was detected using an HRP-conjugated mouse-anti-human IgG mAb (Jackson
454 ImmunoResearch).
455
456 *BW5147 cell flow cytometry:* BW5147 cells were harvested by centrifugation at 900 g and RT
457 from the suspension culture. $1x10^6$ cells were stained with PE- or FITC-conjugated anti-
458 human FcγR mAbs (BD) or a PE-TexasRed-conjugated human IgG-Fc fragment (Rockland)
459 for 1h at 4°C in PBS/3%FCS. After 3 washing steps in PBS/3%FCS, the cells were
460 transferred to Flow cytometry tubes (BD) and analysed using BD LSR Fortessa and FlowJo
461 (V10) software.
462
463 *NK cell activation flow cytometry:* PBMC were purified from donor blood using Lymphocyte
464 separation Media (Anprotec). Primary NK cells were separated from donor PBMCs via
465 magnetic bead negative selection (Stem Cell technologies) and NK cell purity was confirmed

466 via staining of CD3 (Biolegend, clone HIT3a), CD16 (Biolegend, clone 3G8) and CD56
467 (Miltenyi Biotec, clone AF12-7H3). 96well ELISA plates (Nunc Maxisorp) were pre-treated
468 with PBS/10% FCS (v/v) for 1 h at 4°C. NK cells were stimulated in pre-treated plates and
469 incubated at 37°C and 5% CO_2 for 4 h. Golgi Plug and Golgi Stop solutions (BD) were added
470 as suggested by supplier. CD107a (APC, BD, H4A3) specific conjugated mAb was added at
471 the beginning of the incubation period. Following the stimulation period, MIP-1β (PE, BD
472 Pharmigen), IFNγ (BV-510, Biolegends, 4SB3) and TNFα (PE/Cy7, Biolegends, MAB11)
473 production was measured via intracellular staining Cytokines (BD, CytoFix/CytoPerm, Kit as
474 suggested by the supplier). 50 ng/ml PMA (InvivoGen) + 0.5 µM Ionomycin (InvivoGen)
475 were used as a positive stimulation control for NK cell activation. After 3 washing steps in
476 PBS/3%FCS, the cells were transferred to Flow cytometry tubes (BD) and analysed using a
477 BD FACS Fortessa and FlowJo (V10) software. FcγRII or FcγRIII block was performed by
478 addition of receptor specific mAbs (Stem cell technologies, IV.3 and 3G8) at a 1:100 dilution
479 at the beginning of the incubation period. Cells were transferred to Flow cytometry tubes
480 (BD) and analyzed using BD LSR Fortessa and FlowJo (V10) software.
481
482 *Asymmetric flow field flow fractionation (AF4):* The AF4 system consisted of a flow
483 controller (Eclipse AF4, Wyatt), a MALS detector (DAWN Heleos II, Wyatt), a UV detector
484 (1260 Infinity G1314F, Agilent) and the separation channel (SC channel, PES membrane, cut-
485 off 10 kDa, 490 µm spacer, wide type, Wyatt). Elution buffer: 1.15 g/L Na_2HPO_4 (Merck),
486 0.20 g/L NaH_2PO_4 x H_2O (Merck), 8.00 g/L NaCl (Sigma) and 0,20 g/L NaN_3 (Sigma),
487 adjusted to pH 7.4, filtered through 0.1 µm. AF4 sequence (Vx = cross flow in mL/min): (a)
488 elution (2 min, Vx: 1.0); (b) focus (1 min, Vx: 1.0), focus + inject (1 min, Vx: 1.0, inject flow:
489 0.2 mL/min), repeated three times; (c) elution (30 min, linear Vx gradient: 1.0 to 0.0); (d)
490 elution (15 min, Vx: 0.0); (e) elution + inject (5 min, Vx: 0.0). A total protein mass of 17±0.3
491 µg (Ifx, rhTNFα or ICs, respectively) was injected. The eluted sample concentration was

492 calculated from the UV signal at 280 nm using extinction coefficients of 1.240 mL/(mg cm)
493 or 1.450 mL/(mg cm) in the case of TNFα or Ifx, respectively. For the ICs, extinction
494 coefficients were not available and difficult to calculate as the exact stoichiometry is not
495 known. An extinction coefficient of 1.450 mL/(mg cm) was used for calculating the molar
496 masses of all ICs. Especially in the case of ICs rich in TNFα, the true coefficients should be
497 lower, and the molar masses of these complexes are overestimated by not more than 14 %.
498 The determined molar masses for TNFα-rich complexes are therefore biased but the observed
499 variations in molar mass for the different ICs remain valid. The mass-weighted mean of the
500 distribution of molar masses for each sample was calculated using the ASTRA 7 software
501 package (Wyatt).
502
503 *SLE patient cohort:* Sera from patients with SLE were obtained from the Immunologic,
504 Rheumatologic Biobank (IR-B) of the Department of Rheumatology and Clinical
505 Immunology. Biobanking and the project were approved by the local ethical committee of the
506 University of Freiburg (votes 507/16 and 624/14). All patients who provided blood to the
507 biobank had provided written informed consent. Ethical Statement: The study was designed in
508 accordance with the guidelines of the Declaration of Helsinki (revised 2013). Patients with
509 SLE (n = 25) and healthy controls (n = 4) were examined. All patients met the revised ACR
510 classification criteria for SLE. Disease activity was assessed using the SLEDAI-2K score.
511 C3d levels were analyzed in EDTA plasma using rocket double decker immune-
512 electrophoresis with antisera against C3d (Polyclonal Rabbit Anti-Human C3d Complement,
513 Agilent) and C3c (Polyclonal Rabbit Anti-Human C3c Complement Agilent) as previously
514 described (*72*). Anti-human dsDNA antibodies titers were determined in serum using an anti-
515 dsDNA IgG ELISA kit (diagnostik-a GmbH).
516

517 *Patient serum IC precipitation:* For polyethylene glycol (PEG) precipitation human sera were
518 mixed with PEG 6000 (Sigma-Aldrich) in PBS at a final concentration of 10% PEG 6000.
519 After overnight incubation at 4°C, ICs were precipitated by centrifugation at 2000 x g for
520 30 min at 4 °C, pellets were washed once with PEG 6000 and then centrifugated at 2000 x g
521 for 20 min at 4 °C. Supernatants were harvested and precipitates re-suspended in pre-warmed
522 PBS for 1 h at 37 °C. IgG concentrations of serum, precipitates and supernatants obtained
523 after precipitation were quantified by Nanodrop (Thermo Scientific™) measurement.
524
525 *Mice and Models:* Animal experiments were approved by the local governmental commission
526 for animal protection of Freiburg (Regierungspräsidium Freiburg, approval no. G16/59 and
527 G19/21). Lupus-prone (NZBxNZW)F1 mice (NZB/WF1) were generated by crossing
528 NZB/BlNJ mice with NZW/LacJ mice, purchased from The Jackson Laboratory. KRNtg mice
529 were obtained from F. Nimmerjahn (Universität Erlangen-Nürnberg) with the permission of
530 D. Mathis and C. Benoist (Harvard Medical School, Boston, MA), C57BL/6 mice (BL/6) and
531 NOD/ShiLtJArc (NOD/Lt) mice were obtained from the Charles River Laboratories. K/BxN
532 (KRNtgxNOD)F1 mice (K/BxN) were obtained by crossing KRNtg mice and NOD/Lt mice.
533 All mice were housed in a 12-h light/dark cycle, with food and water ad libitum. Mice were
534 euthanized and blood collected for serum preparation from 16 weeks old BL/6 animals, from
535 16 weeks old arthritic K/BxN animals and from 26 – 38 weeks old NZB/WF1 mice with
536 established glomerulonephritis.
537
538 *Statistical analyses:* Statistical analyses were performed using Graphpad Prism software (v6)
539 and appropriate tests.
540
541
542

543 **Supplementary Materials**

544 Fig. S1. rhTNFα is not toxic to mouse lymphocyte BW5147 cells even at high concentrations.

545 Fig. S2. AF4 elution profiles of Ifx/TNFα-immune complexes.

546 Table S1. Analysis of the molar mass distribution of ICs from AF4 data.

547 **References**

548 1. L. L. Lu, T. J. Suscovich, S. M. Fortune, G. Alter, Beyond binding: antibody effector
549 functions in infectious diseases. *Nat Rev Immunol* **18**, 46-61 (2018).
550 2. J. V. Ravetch, S. Bolland, IgG Fc receptors. *Annu Rev Immunol* **19**, 275-290 (2001).
551 3. C. E. van der Poel, R. M. Spaapen, J. G. van de Winkel, J. H. Leusen, Functional
552 characteristics of the high affinity IgG receptor, FcgammaRI. *J Immunol* **186**, 2699-
553 2704 (2011).
554 4. P. Bruhns *et al.*, Specificity and affinity of human Fcgamma receptors and their
555 polymorphic variants for human IgG subclasses. *Blood* **113**, 3716-3725 (2009).
556 5. D. Urlaub *et al.*, Activation of natural killer cells by rituximab in granulomatosis with
557 polyangiitis. *Arthritis Res Ther* **21**, 277 (2019).
558 6. A. Lux, X. Yu, C. N. Scanlan, F. Nimmerjahn, Impact of immune complex size and
559 glycosylation on IgG binding to human FcgammaRs. *J Immunol* **190**, 4315-4323
560 (2013).
561 7. F. Kiefer *et al.*, The Syk protein tyrosine kinase is essential for Fc gamma receptor
562 signaling in macrophages and neutrophils. *Mol Cell Biol* **18**, 4209-4220 (1998).
563 8. Y. Luo, J. W. Pollard, A. Casadevall, Fcgamma receptor cross-linking stimulates cell
564 proliferation of macrophages via the ERK pathway. *J Biol Chem* **285**, 4232-4242
565 (2010).
566 9. S. Greenberg, P. Chang, S. C. Silverstein, Tyrosine phosphorylation of the gamma
567 subunit of Fc gamma receptors, p72syk, and paxillin during Fc receptor-mediated
568 phagocytosis in macrophages. *J Biol Chem* **269**, 3897-3902 (1994).
569 10. S. Bournazos, T. T. Wang, R. Dahan, J. Maamary, J. V. Ravetch, Signaling by
570 Antibodies: Recent Progress. *Annu Rev Immunol* **35**, 285-311 (2017).
571 11. F. Nimmerjahn, J. V. Ravetch, Antibody-mediated modulation of immune responses.
572 *Immunol Rev* **236**, 265-275 (2010).
573 12. M. Heidelberger, F. E. Kendall, A Quantitative Study of the Precipitin Reaction
574 between Type Iii Pneumococcus Polysaccharide and Purified Homologous Antibody.
575 *J Exp Med* **50**, 809-823 (1929).
576 13. M. Heidelberger, F. E. Kendall, The Precipitin Reaction between Type Iii
577 Pneumococcus Polysaccharide and Homologous Antibody : Iii. A Quantitative Study
578 and a Theory of the Reaction Mechanism. *J Exp Med* **61**, 563-591 (1935).
579 14. A. M. Duchemin, L. K. Ernst, C. L. Anderson, Clustering of the High-Affinity Fc
580 Receptor for Immunoglobulin-G (Fc-Gamma-Ri) Results in Phosphorylation of Its
581 Associated Gamma-Chain. *J Biol Chem* **269**, 12111-12117 (1994).
582 15. A. Getahun, J. C. Cambier, Of ITIMs, ITAMs, and ITAMis: revisiting immunoglobulin
583 Fc receptor signaling. *Immunol Rev* **268**, 66-73 (2015).
584 16. P. Bruhns, F. Jonsson, Mouse and human FcR effector functions. *Immunol Rev* **268**,
585 25-51 (2015).
586 17. P. Bruhns, Properties of mouse and human IgG receptors and their contribution to
587 disease models. *Blood* **119**, 5640-5649 (2012).
588 18. F. Nimmerjahn, J. V. Ravetch, Fcgamma receptors as regulators of immune
589 responses. *Nat Rev Immunol* **8**, 34-47 (2008).
590 19. F. Nimmerjahn, J. V. Ravetch, Fcgamma receptors: old friends and new family
591 members. *Immunity* **24**, 19-28 (2006).
592 20. M. Guilliams, P. Bruhns, Y. Saeys, H. Hammad, B. N. Lambrecht, The function of
593 Fcgamma receptors in dendritic cells and macrophages. *Nat Rev Immunol* **14**, 94-108
594 (2014).
595 21. Z. K. Indik *et al.*, The high affinity Fc gamma receptor (CD64) induces phagocytosis in
596 the absence of its cytoplasmic domain: the gamma subunit of Fc gamma RIIIA
597 imparts phagocytic function to Fc gamma RI. *Exp Hematol* **22**, 599-606 (1994).
598 22. G. Fossati, R. C. Bucknall, S. W. Edwards, Insoluble and soluble immune complexes
599 activate neutrophils by distinct activation mechanisms: changes in functional
600 responses induced by priming with cytokines. *Ann Rheum Dis* **61**, 13-19 (2002).

601 23. J. J. Hubbard *et al.*, FcRn is a CD32a coreceptor that determines susceptibility to IgG
602 immune complex-driven autoimmunity. *J Exp Med* **217**, (2020).
603 24. A. Pincetic *et al.*, Type I and type II Fc receptors regulate innate and adaptive
604 immunity. *Nat Immunol* **15**, 707-716 (2014).
605 25. G. Vidarsson, G. Dekkers, T. Rispens, IgG subclasses and allotypes: from structure
606 to effector functions. *Front Immunol* **5**, 520 (2014).
607 26. M. Z. Tay, K. Wiehe, J. Pollara, Antibody-Dependent Cellular Phagocytosis in
608 Antiviral Immune Responses. *Front Immunol* **10**, 332 (2019).
609 27. E. A. Laborde *et al.*, Immune complexes inhibit differentiation, maturation, and
610 function of human monocyte-derived dendritic cells. *J Immunol* **179**, 673-681 (2007).
611 28. S. Kang *et al.*, IgG-Immune Complexes Promote B Cell Memory by Inducing BAFF. *J*
612 *Immunol* **196**, 196-206 (2016).
613 29. V. Granger, M. Peyneau, S. Chollet-Martin, L. de Chaisemartin, Neutrophil
614 Extracellular Traps in Autoimmunity and Allergy: Immune Complexes at Work. *Front*
615 *Immunol* **10**, 2824 (2019).
616 30. S. Berger, H. Ballo, H. J. Stutte, Immune complex-induced interleukin-6, interleukin-
617 10 and prostaglandin secretion by human monocytes: A network of pro- and anti-
618 inflammatory cytokines dependent on the antigen:antibody ratio. *Eur J Immunol* **26**,
619 1297-1301 (1996).
620 31. L. Koenderman, Inside-Out Control of Fc-Receptors. *Front Immunol* **10**, 544 (2019).
621 32. R. Plomp *et al.*, Subclass-specific IgG glycosylation is associated with markers of
622 inflammation and metabolic health. *Sci Rep* **7**, 12325 (2017).
623 33. T. C. Pierson *et al.*, The stoichiometry of antibody-mediated neutralization and
624 enhancement of West Nile virus infection. *Cell Host Microbe* **1**, 135-145 (2007).
625 34. K. R. Patel, J. T. Roberts, A. W. Barb, Multiple Variables at the Leukocyte Cell
626 Surface Impact Fc gamma Receptor-Dependent Mechanisms. *Front Immunol* **10**, 223
627 (2019).
628 35. S. Bohm, D. Kao, F. Nimmerjahn, Sweet and sour: the role of glycosylation for the
629 anti-inflammatory activity of immunoglobulin G. *Current topics in microbiology and*
630 *immunology* **382**, 393-417 (2014).
631 36. R. J. Stopforth *et al.*, Detection of Experimental and Clinical Immune Complexes by
632 Measuring SHIP-1 Recruitment to the Inhibitory FcgammaRIIB. *J Immunol* **200**, 1937-
633 1950 (2018).
634 37. T. T. Wang, J. V. Ravetch, Immune complexes: not just an innocent bystander in
635 chronic viral infection. *Immunity* **42**, 213-215 (2015).
636 38. D. H. Yamada *et al.*, Suppression of Fcgamma-receptor-mediated antibody effector
637 function during persistent viral infection. *Immunity* **42**, 379-390 (2015).
638 39. U. Antes, H. P. Heinz, D. Schultz, D. Brackertz, M. Loos, C1q-bearing immune
639 complexes detected by a monoclonal antibody to human C1q in rheumatoid arthritis
640 sera and synovial fluids. *Rheumatol Int* **10**, 245-250 (1991).
641 40. R. H. Zubler *et al.*, Circulating and intra-articular immune complexes in patients with
642 rheumatoid arthritis. Correlation of 125I-Clq binding activity with clinical and biological
643 features of the disease. *J Clin Invest* **57**, 1308-1319 (1976).
644 41. D. Koffler, V. Agnello, R. Thoburn, H. G. Kunkel, Systemic lupus erythematosus:
645 prototype of immune complex nephritis in man. *J Exp Med* **134**, 169-179 (1971).
646 42. T. V. Rajan, The Gell-Coombs classification of hypersensitivity reactions: a re-
647 interpretation. *Trends in immunology* **24**, 376-379 (2003).
648 43. S. Tahir *et al.*, A CD153+CD4+ T follicular cell population with cell-senescence
649 features plays a crucial role in lupus pathogenesis via osteopontin production. *J*
650 *Immunol* **194**, 5725-5735 (2015).
651 44. A. Bano *et al.*, CD28 (null) CD4 T-cell expansions in autoimmune disease suggest a
652 link with cytomegalovirus infection. *F1000Res* **8**, (2019).
653 45. E. Corrales-Aguilar *et al.*, A novel assay for detecting virus-specific antibodies
654 triggering activation of Fcgamma receptors. *Journal of immunological methods* **387**,
655 21-35 (2013).

656 46. H. A. D. Lagasse, H. Hengel, B. Golding, Z. E. Sauna, Fc-Fusion Drugs Have
657 FcgammaR/C1q Binding and Signaling Properties That May Affect Their
658 Immunogenicity. *AAPS J* **21**, 62 (2019).
659 47. S. Van den Hoecke *et al.*, Hierarchical and Redundant Roles of Activating
660 FcgammaRs in Protection against Influenza Disease by M2e-Specific IgG1 and
661 IgG2a Antibodies. *J Virol* **91**, (2017).
662 48. M. Tanaka *et al.*, Activation of Fc gamma RI on monocytes triggers differentiation into
663 immature dendritic cells that induce autoreactive T cell responses. *J Immunol* **183**,
664 2349-2355 (2009).
665 49. S. Lisi, M. Sisto, D. D. Lofrumento, S. D'Amore, M. D'Amore, Advances in the
666 understanding of the Fc gamma receptors-mediated autoantibodies uptake. *Clin Exp*
667 *Med* **11**, 1-10 (2011).
668 50. J. C. Anania, A. M. Chenoweth, B. D. Wines, P. M. Hogarth, The Human
669 FcgammaRII (CD32) Family of Leukocyte FcR in Health and Disease. *Front Immunol*
670 **10**, 464 (2019).
671 51. D. Metes *et al.*, Expression of functional CD32 molecules on human NK cells is
672 determined by an allelic polymorphism of the FcgammaRIIC gene. *Blood* **91**, 2369-
673 2380 (1998).
674 52. W. B. Breunis *et al.*, Copy number variation of the activating FCGR2C gene
675 predisposes to idiopathic thrombocytopenic purpura. *Blood* **111**, 1029-1038 (2008).
676 53. F. Vuckovic *et al.*, Association of systemic lupus erythematosus with decreased
677 immunosuppressive potential of the IgG glycome. *Arthritis Rheumatol* **67**, 2978-2989
678 (2015).
679 54. Y. Kaneko, F. Nimmerjahn, J. V. Ravetch, Anti-inflammatory activity of
680 immunoglobulin G resulting from Fc sialylation. *Science* **313**, 670-673 (2006).
681 55. P. Kolb *et al.*, Identification and Functional Characterization of a Novel Fc Gamma-
682 Binding Glycoprotein in Rhesus Cytomegalovirus. *J Virol* **93**, (2019).
683 56. U. E. Nydegger, J. S. t. Davis, Soluble immune complexes in human disease. *CRC*
684 *Crit Rev Clin Lab Sci* **12**, 123-170 (1980).
685 57. R. J. Levinsky, J. S. Cameron, J. F. Soothill, Serum immune complexes and disease
686 activity in lupus nephritis. *Lancet* **1**, 564-567 (1977).
687 58. R. J. Levinsky, Role of circulating soluble immune complexes in disease. *Arch Dis*
688 *Child* **53**, 96-99 (1978).
689 59. L. Briant, N. Coudronniere, V. Robert-Hebmann, M. Benkirane, C. Devaux, Binding of
690 HIV-1 virions or gp120-anti-gp120 immune complexes to HIV-1-infected quiescent
691 peripheral blood mononuclear cells reveals latent infection. *J Immunol* **156**, 3994-
692 4004 (1996).
693 60. S. K. Oh *et al.*, Identification of HIV-1 envelope glycoprotein in the serum of AIDS and
694 ARC patients. *J Acquir Immune Defic Syndr (1988)* **5**, 251-256 (1992).
695 61. D. A. Vuitton, L. Vuitton, E. Seilles, P. Galanaud, A plea for the pathogenic role of
696 immune complexes in severe Covid-19. *Clin Immunol* **217**, 108493 (2020).
697 62. K. Madalinski, B. Burczynska, K. H. Heermann, A. Uy, W. H. Gerlich, Analysis of viral
698 proteins in circulating immune complexes from chronic carriers of hepatitis B virus.
699 *Clin Exp Immunol* **84**, 493-500 (1991).
700 63. D. A. Wetter, M. D. Davis, Lupus-like syndrome attributable to anti-tumor necrosis
701 factor alpha therapy in 14 patients during an 8-year period at Mayo Clinic. *Mayo Clin*
702 *Proc* **84**, 979-984 (2009).
703 64. D. A. MacDonald *et al.*, Aflibercept exhibits VEGF binding stoichiometry distinct from
704 bevacizumab and does not support formation of immune-like complexes.
705 *Angiogenesis* **19**, 389-406 (2016).
706 65. K. O. Saunders, Conceptual Approaches to Modulating Antibody Effector Functions
707 and Circulation Half-Life. *Front Immunol* **10**, 1296 (2019).
708 66. T. Li *et al.*, Modulating IgG effector function by Fc glycan engineering. *Proceedings of*
709 *the National Academy of Sciences of the United States of America* **114**, 3485-3490
710 (2017).

711 67. M. R. Goodier *et al.*, Sustained Immune Complex-Mediated Reduction in CD16
712 Expression after Vaccination Regulates NK Cell Function. *Front Immunol* **7**, 384
713 (2016).
714 68. T. N. Mayadas, G. C. Tsokos, N. Tsuboi, Mechanisms of immune complex-mediated
715 neutrophil recruitment and tissue injury. *Circulation* **120**, 2012-2024 (2009).
716 69. S. Nagarajan *et al.*, Cell-specific, activation-dependent regulation of neutrophil
717 CD32A ligand-binding function. *Blood* **95**, 1069-1077 (2000).
718 70. K. Morizono *et al.*, Redirecting lentiviral vectors pseudotyped with Sindbis virus-
719 derived envelope proteins to DC-SIGN by modification of N-linked glycans of
720 envelope proteins. *J Virol* **84**, 6923-6934 (2010).
721 71. E. Corrales-Aguilar *et al.*, Human cytomegalovirus Fcgamma binding proteins gp34
722 and gp68 antagonize Fcgamma receptors I, II and III. *PLoS pathogens* **10**, e1004131
723 (2014).
724 72. E. Rother, B. Lang, R. Coldewey, K. Hartung, H. H. Peter, Complement split product
725 C3d as an indicator of disease activity in systemic lupus erythematosus. *Clin*
726 *Rheumatol* **12**, 31-35 (1993).

727

728

Acknowledgements: We thank T. Schleyer (IR-B Biobank) for providing patient samples. We are indebted to Falk. Nimmerjahn (Universität Erlangen-Nürnberg) for providing KRNtg mice. **Funding:** This work was supported by an intramural junior investigator fund of the Faculty of Medicine to PK (EQUIP - Funding for Medical Scientists, Faculty of Medicine, University of Freiburg), by the German Research foundation (DFG) (FOR2830 HE 2526/9-1) to HH, by the DFG research grant TRR130 to REV and the Ministry of Science, Research, and Arts Baden-Württemberg (Margarete von Wrangell Programm) to NC. **Author contributions:** HC and PK designed and developed the reporter system, conducted Fc-gamma receptor activation experiments and prepared synthetic immune complexes. AMP, US and REV manage the SLE patient cohort, provided sera and performed immune complex precipitation as well as IgG quantification. MH designed and performed AF4 analyses. NC manages the mouse models and provided sera. HH and PK supervised all experiments. HC and PK analysed and interpreted data. PK wrote the paper assisted by HC, AMP, MH, NC, REV and HH. **Competing interests:** The authors declare no financial and non-financial competing interests. **Data and materials availability:** All data associated with this study are present in the paper or Supplementary Materials.

746 **Figures**

747

748 **Figure 1**

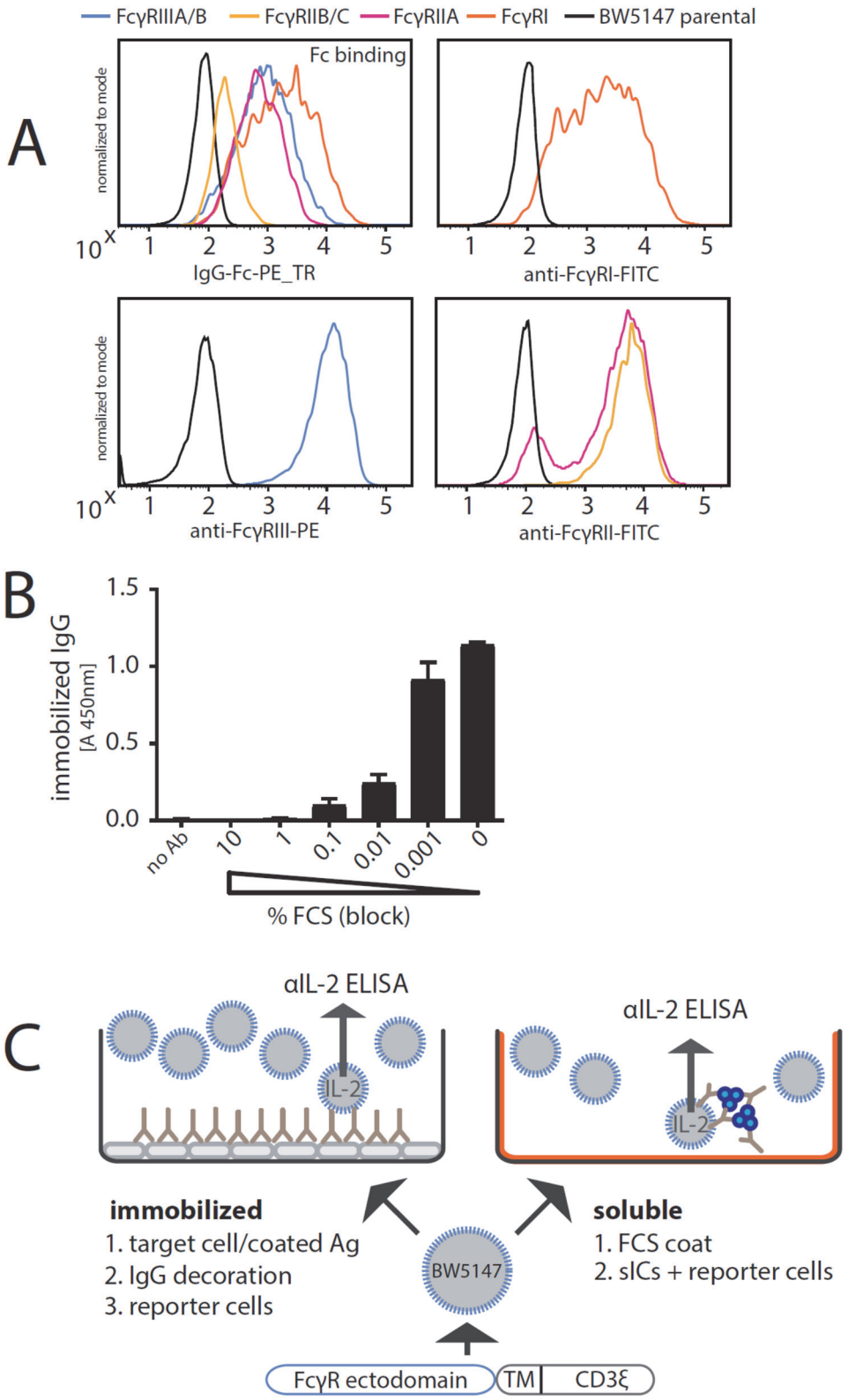

749

750

751 **Fig. 1. Establishment of a cell-based reporter assay measuring FcγR activation in**
752 **response to sICs.** A) BW5147 reporter cells stably expressing human FcγR-ζ chain chimeras
753 or BW5147 parental cells were stained with FcγR specific conjugated mAbs as indicated and
754 measured for surface expression of FcγRs via flow cytometry. Fcγ binding was determined
755 using a PE-TexasRed-conjugated human IgG-Fc fragment. B) FCS coating of an ELISA
756 microtiter plate allows for suspension of subsequently added IgG. Plate bound IgG was
757 quantified via ELISA. PBS supplemented with >1% FCS (v/v) avoids adhesion of IgG
758 (rituximab, Rtx) to the ELISA plate. C) Schematic of an immobilized IC or soluble IC setup.
759 BW5147 reporter cells expressing chimeric human FcγR receptors secrete IL-2 in response to
760 FcγR activation by clustered IgG. Soluble ICs are generated using mAbs and multivalent
761 antigens (blue). Solubility is achieved by pre-blocking an ELISA plate using PBS
762 supplemented with 10% FCS (FCS coat, orange).
763

764 **Figure 2**

765

766

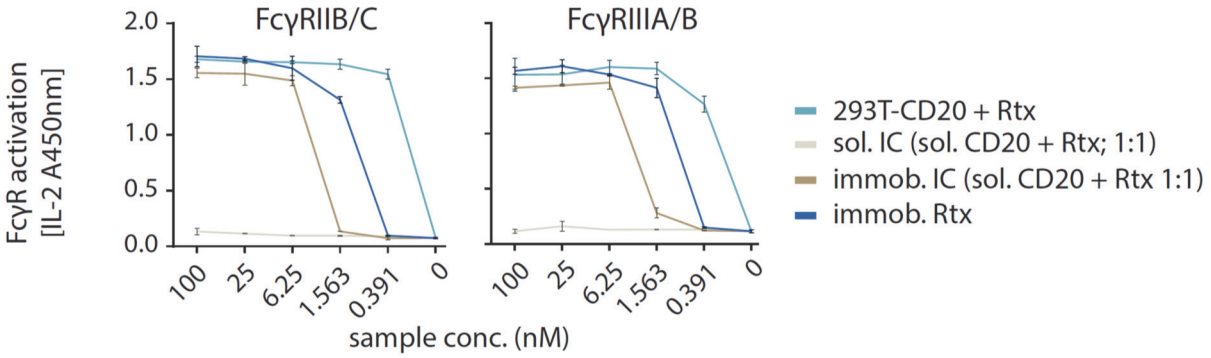

767

768

769 **Fig. 2. FcγRIIB/C and FcγRIIIA/B do not respond to small hetero-dimeric sICs but are**
770 **sensitive to immobilized IgG/ICs.** Dose-dependent activation of FcγR-bearing reporter cells
771 by immobilized IC can be mimicked by immobilized IgG. Response curves of human
772 FcγRIIB/C and FcγRIIIA/B are similar between opsonized cells (293T cells stably expressing
773 CD20 + Rtx), immobilized IC (rec. soluble CD20 + Rtx) and immobilized IgG (Rtx). sIC
774 formed by monovalent antigen (rec. soluble CD20) do not activate human FcγRs. X-Axis
775 shows sample concentration determined by antibody molarity. Y-Axis shows FcγR activation
776 determined by reporter cell IL-2 production.

777

778 **Figure 3**

779

780

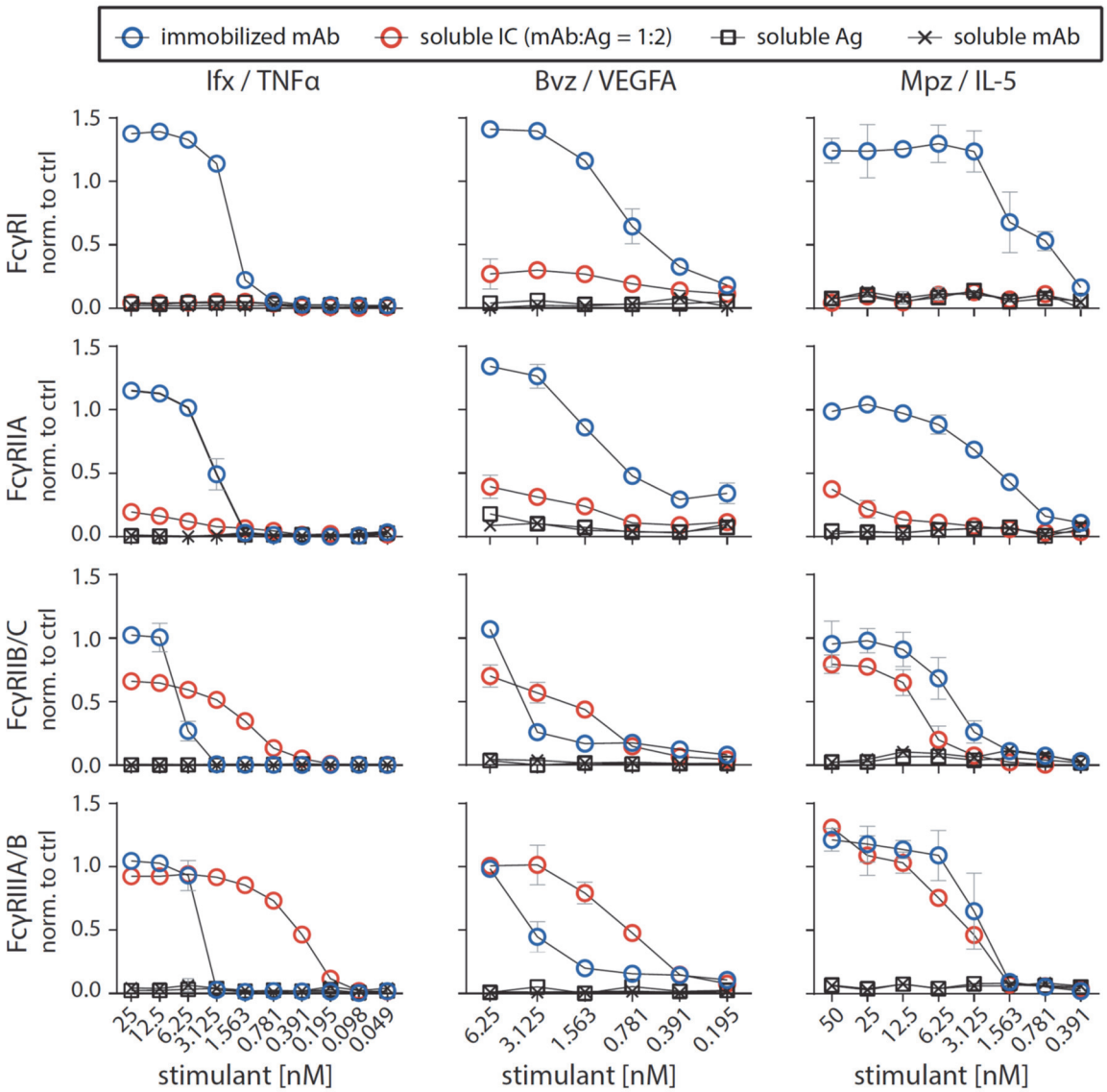

781

782

783 **Fig. 3. FcγRIIB/C and FcγRIIIA/B are activated by sICs formed from multivalent**
784 **antigens.** Three different multivalent ultra-pure antigens (Ag) mixed with respective therapy-
785 grade mAbs were used to generate sICs as indicated for each set of graphs (top to bottom). IC
786 pairs: infliximab (Ifx) and rhTNFα; mepolizumab (Mpz) and rhIL-5; bevacizumab (Bvz) and
787 rhVEGFA. X-Axis: concentrations of stimulant expressed as molarity of either mAb or Ag
788 monomer and IC (expressed as mAb molarity) at a mAb:Ag ratio of 1:2. Soluble antigen or
789 soluble antibody alone served as negative controls and were not sufficient to activate human
790 FcγRs. FcγR responses were normalized to immobilized rituximab (Rtx) at 1µg/well (set to 1)
791 and a medium control (set to 0). All FcγRs show dose-dependent activation towards
792 immobilized IgG. FcγRIIA shows low activation at high sIC concentrations compared to
793 immobilized IgG activation. FcγRI shows no activation towards sICs. FcγRIIIA/B and
794 FcγRIIB/C are dose-dependently activated by sICs with responses comparable in strength to
795 immobilized IgG stimulant. Experiments performed in technical replicates. Error bars = SD.
796 Error bars smaller than symbols are not shown.

797 **Figure 4**

798

799

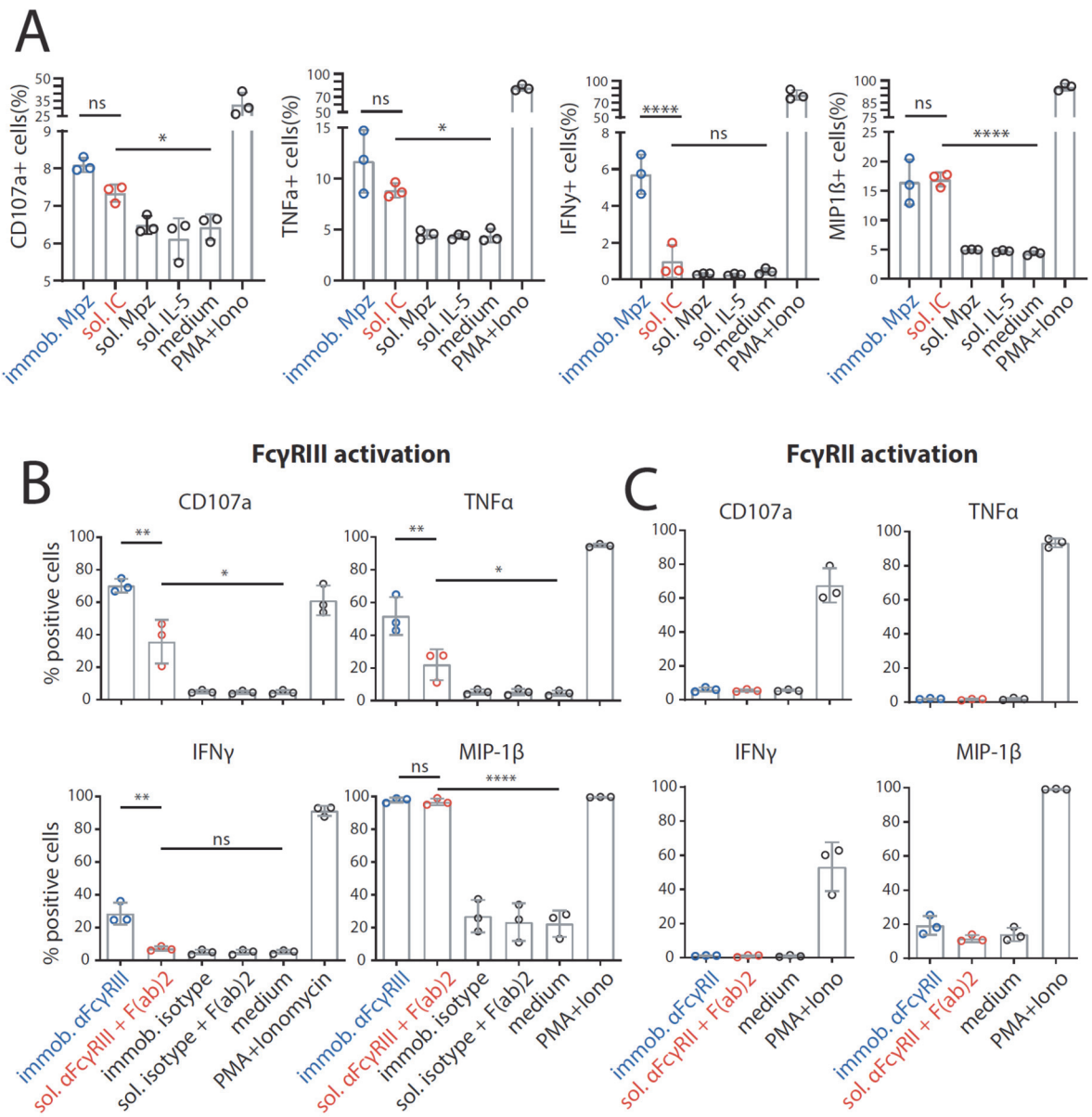

800

801

802

803 **Fig. 4. The FcγRIII-dependent activation pattern of primary NK cells depends on IC**
804 **solubility**. Negatively selected primary NK cells purified from PBMCs of three healthy
805 donors were tested for NK cell activation markers. Error bars = SD. Two-way ANOVA
806 (Turkey). A) NK cells were incubated with immobilized IgG (mepolizumab, Mpz), soluble IC
807 (Mpz:IL-5 = 1:1), soluble Mpz or soluble IL-5 (all at 200 nM, 10^6 cells). Incubation with
808 PMA and Ionomycin (Iono) served as a positive control. Incubation with medium alone
809 served as a negative control. B) NK cells were incubated for 4 h with immobilized FcγRIII-
810 specific mAb, soluble mouse-anti-human IgG $F(ab)_2$ complexed FcγRIII-specific mAb
811 (reverse sICs), immobilized IgG of non-FcγRIII-specificity (isotype control) or soluble $F(ab)_2$
812 complexed isotype control (all at 1µg, 10^6 cells). Incubation with PMA and Ionomycin served
813 as a positive control. Incubation with medium alone served as a negative control. C) As in B
814 using an FcγRII-specific mAb. NK cells from the tested donors in this study do not react to
815 FcγRII activation.

816 **Figure 5**

817

818

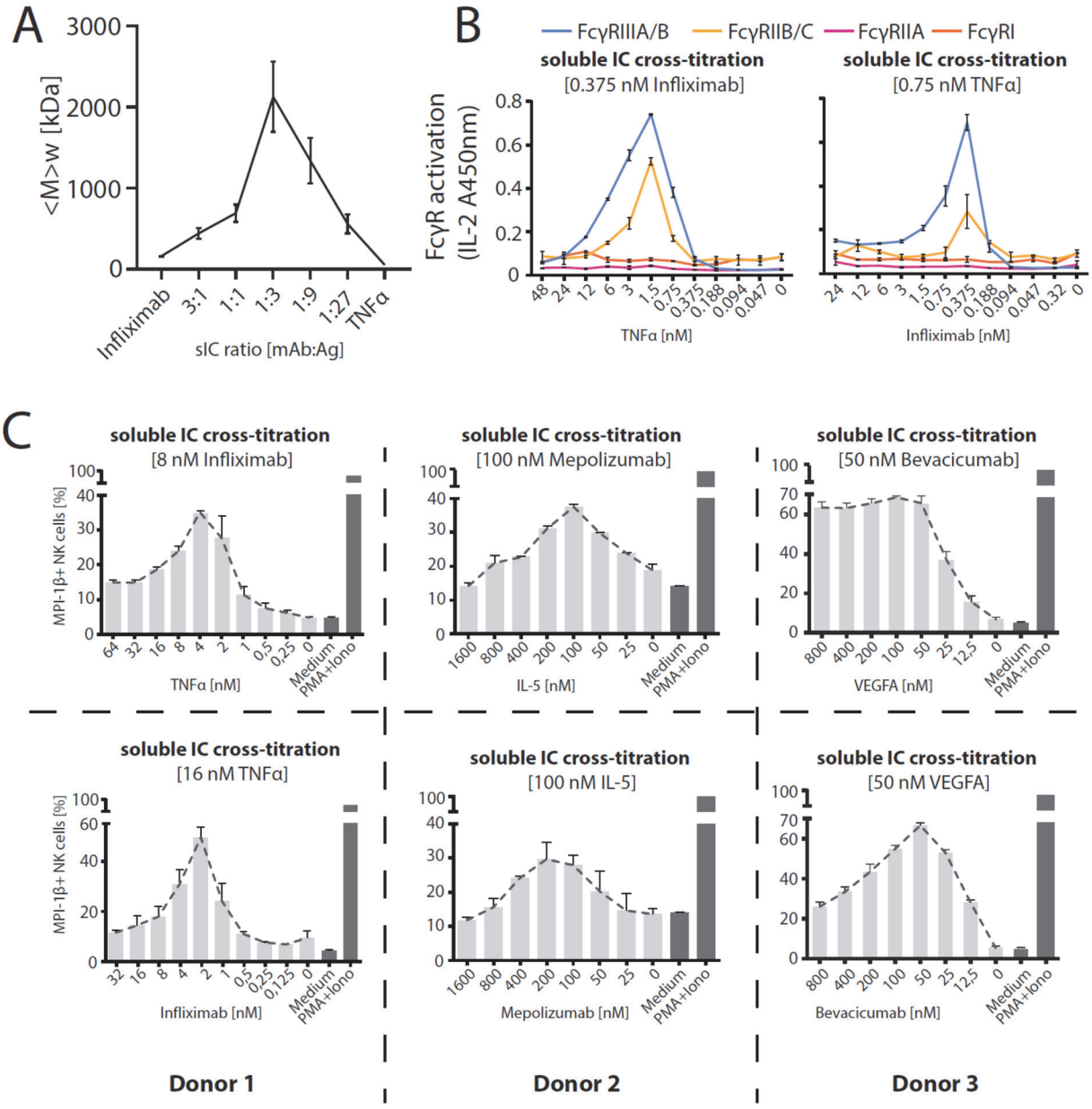

819

820

821 **Fig. 5. FcγRIIB/C and FcγR-IIIA/B respond to sIC size reproducing a Heidelberger-**
822 **Kendall like precipitation curve.** A) infliximab (mAb) and rhTNFα (Ag) were mixed at
823 different ratios (17 µg total protein, calculated from monomer molarity) and analysed via
824 AF4. sIC size is maximal at a 1:3 ratio of mAb:Ag and reduced when either mAb or Ag are
825 given in excess. $\langle M \rangle_w$ = mass-weighted mean of the molar mass distribution. Three
826 independent experiments. Error bars = SD. Data taken from Table S1. One complete run
827 analysis is shown in Fig. S2. B) FcγR BW5147 reporter cell activation is sensitive to sIC size.
828 sICs of different size were generated by cross-titration according to the AF4 determination.
829 Reporter cells were incubated with fixed amounts of either mAb (infliximab, left) or Ag
830 (rhTNFα, right) and titrated amounts of antigen or antibody, respectively. X-Axis shows
831 titration of either antigen or antibody, respectively (TNFα calculated as monomer). IL-2
832 production of reporter cells shows a peak for FcγRIIB/C and FcγRIIIA/B activation at an
833 antibody:antigen ratio between 1:2 and 1:4. FcγRs I and IIA show no activation towards sICs
834 in line with previous observations, see Fig.3. Two independent experiments. Error bars = SD.
835 C) Purified primary NK cells from three different donors were incubated with cross-titrated
836 sICs as in A. NK cells were measured for MIP-1β expression (% positivity). Incubation with
837 PMA and Ionomycin served as a positive control. Incubation with medium alone served as a
838 negative control. Measured in technical replicates. Error bars = SD.

839 **Figure 6**

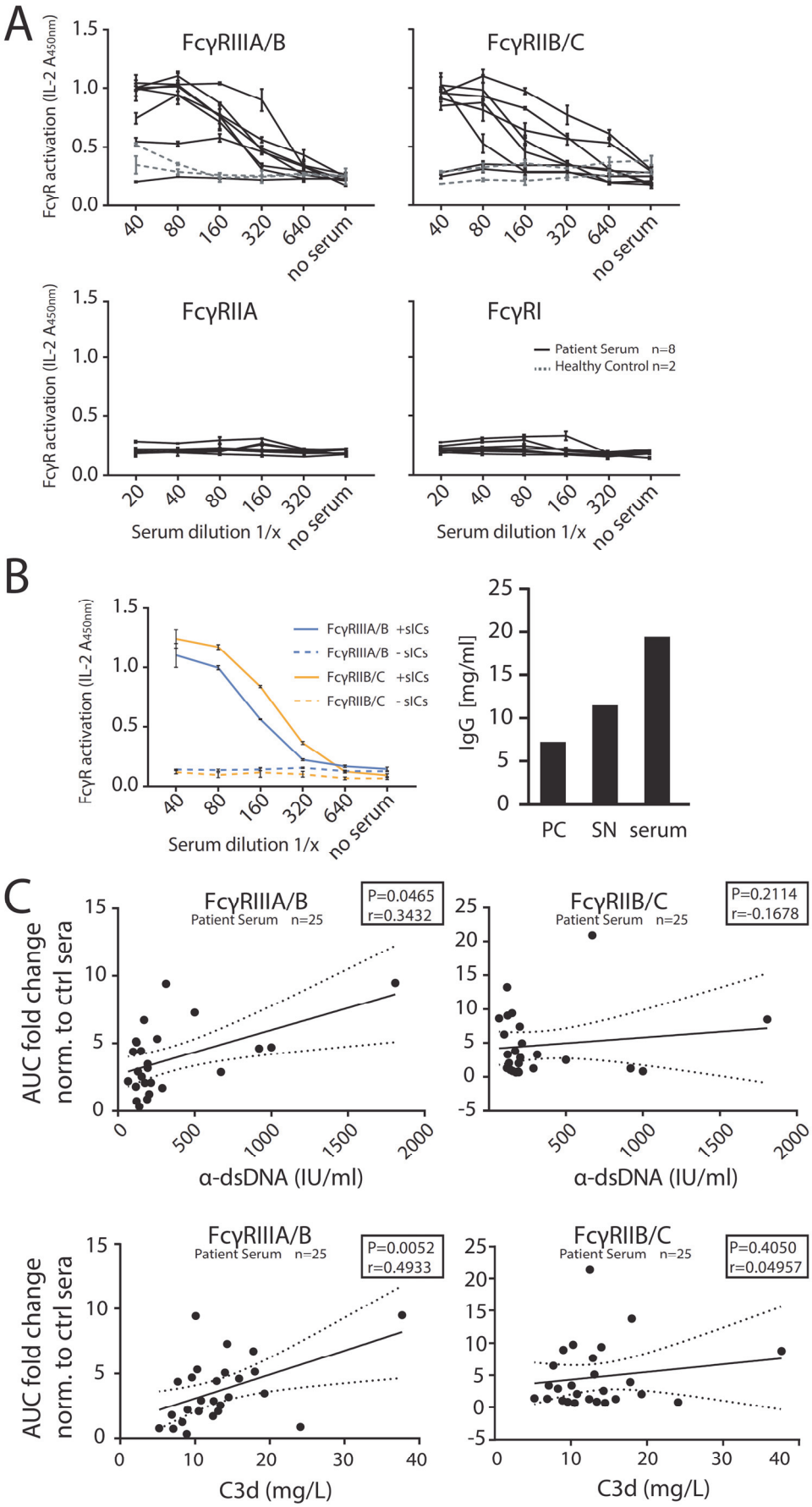

840

841 **Fig. 6. The reporter assay enables quantification of serum-derived sICs from SLE**
842 **patients.** Serum derived sIC from systemic lupus erythematosus (SLE) patients activate
843 human FcγR reporter cells. 25 patients and 4 healthy control individuals were separated into
844 three groups for measurement. A) Experiments shown for an exemplary group of 8 SLE
845 patients and two healthy individuals. Dose-dependent reactivity of FcγRs IIIA/B and IIB/C
846 was observed only for SLE patient sera and not for sera from healthy individuals. FcγRs I and
847 IIA show no reactivity towards clinical IC in line with previous observations. B) Activation of
848 FcγRs IIB/C and IIIA/B by patient serum is mediated by serum derived sICs. Patient serum
849 samples were depleted of sICs by PEG precipitation and the supernatant (SN) was compared
850 to untreated serum regarding FcγR activation (left). Performed in technical replicates. IgG
851 concentration in the precipitate (PC), supernatant (SN) or unfractionated serum respectively is
852 shown in the bar graph (right). IC precipitation did leave non-complexed IgG in the
853 supernatant. C) FcγRIIIA/B activation, but not FcγRIIB/C activation, significantly correlates
854 with known SLE disease markers. FcγR activation data from A was correlated to established
855 SLE disease markers (α-dsDNA levels indicated as IU/ml or C3d concentrations indicated as
856 mg/L). FcγR activation from a dose-response curve as in A was calculated as area under curve
857 (AUC) for each SLE patient (n=25) or healthy individual (n=4) and expressed as fold change
858 compared to the healthy control mean. SLE patients with α-dsDNA levels below 50 IU/ml
859 and C3d values below 6 mg/L were excluded. One-tailed Spearman's.
860
861

862 **Figure 7**

863

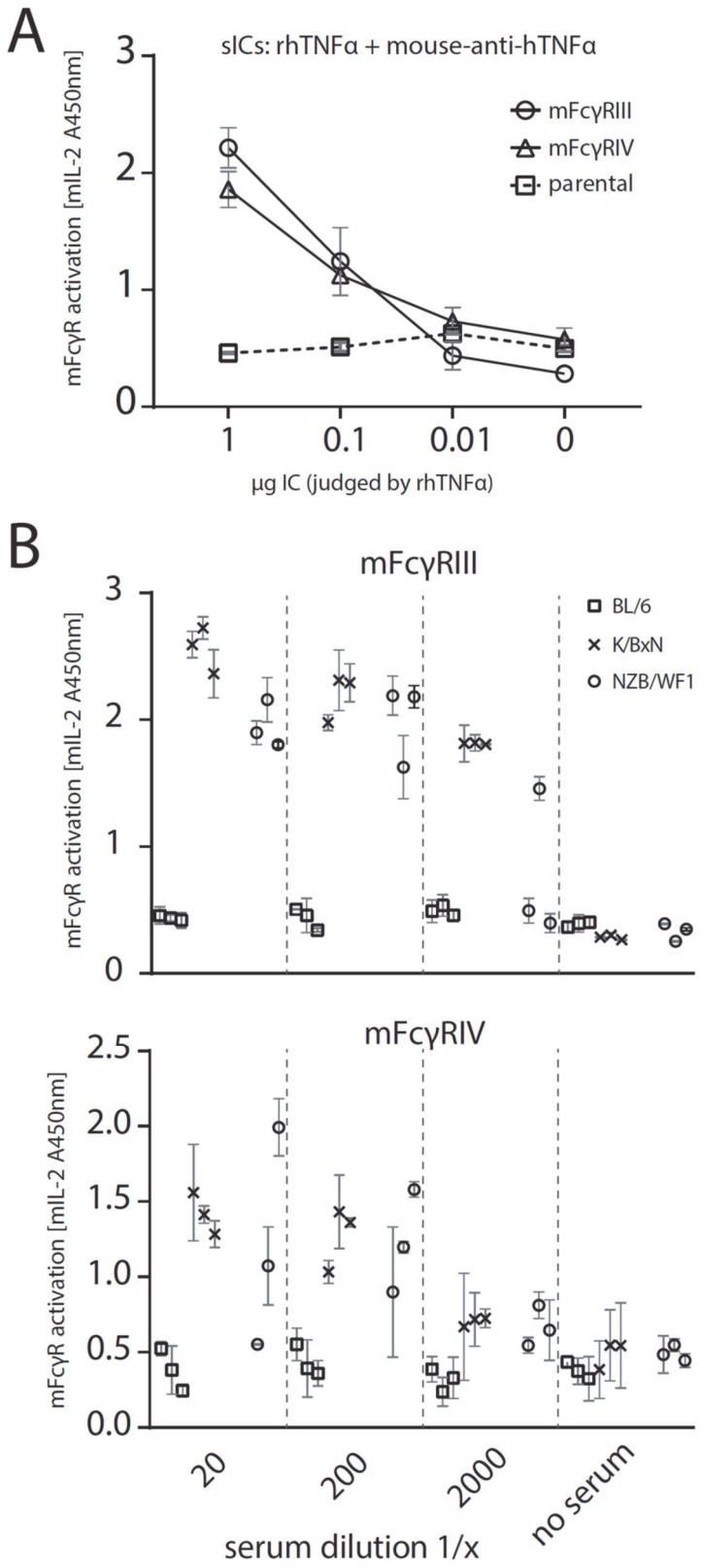

864

865

866 **Fig. 7. The reporter assay can be applied to mouse models of autoimmune disease.** A)
867 Reporter cells expressing mFcγRIII, mFcγRIV or parental BW5147 cells were incubated with
868 titrated amounts of synthetic sICs generated from rhTNFα and mouse-anti-hTNFα at a 1:1
869 ratio by mass. One experiment in technical replicates. Error bars = SD. B) Titrations of 3
870 mouse sera per group (C57BL/6, K/BxN or NZB/WF1) were incubated with mFcγR reporter
871 cells and FcγR activation was assessed as described above. Sera from BL/6 mice served as
872 negative control. Performed in technical replicates. Error bars = SD.
873
874

875 **Supplementary Materials**

876

877 **Figure S1**

878

879

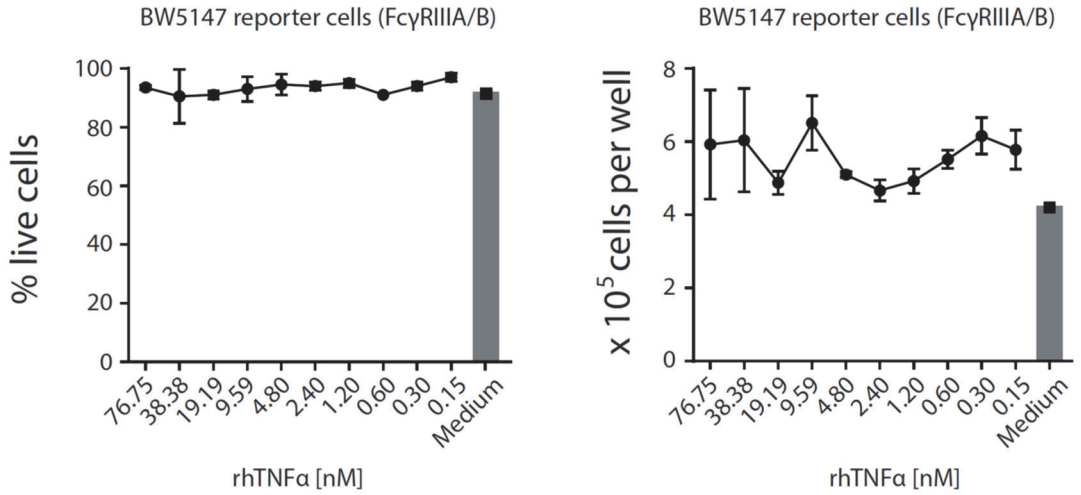

880

881 **Fig. S1. rhTNFα is not toxic to mouse lymphocyte BW5147 cells even at high**
882 **concentrations**. Cell count and percentage of live cells were unaltered over a 16 h time frame
883 of reporter cell culture in the presence of indicated rhTNFα concentrations and comparable to
884 regular growth in complete medium. Experiments were conducted in 3 replicates. Error bars =
885 SD.

886

887 **Figure S2**

888

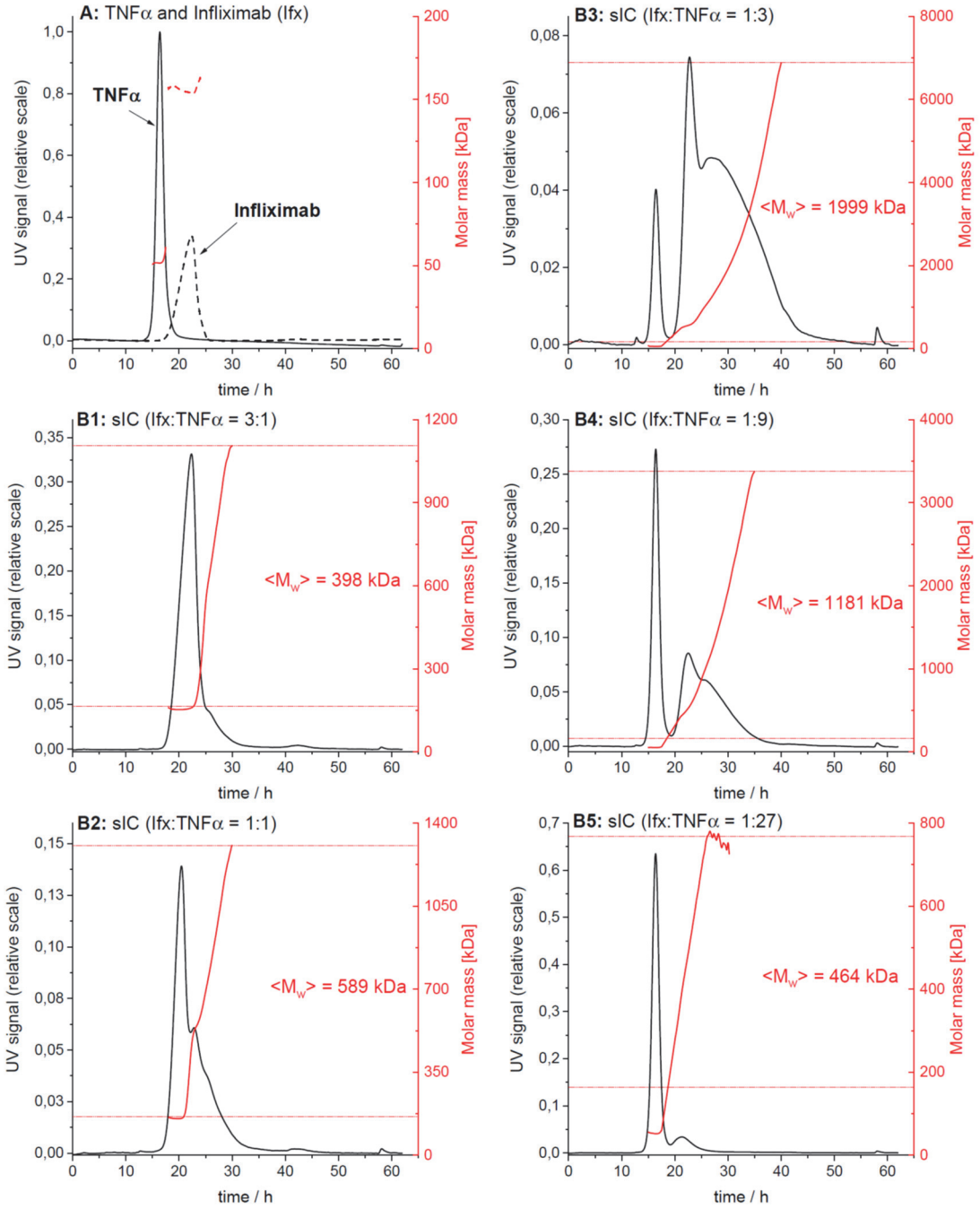

889

890

891 **Fig. S2. AF4 elution profiles of Ifx/TNFα-immune complexes.**

892 The elution profiles from one of three independent runs are shown. Protein concentration in
893 the eluate is shown in black (UV signal at λ = 280 nm, normalized to the highest UV signal
894 found in this experiment), molar masses determined by MALS for a given retention time in
895 red. Horizontal red lines indicate the range of molar masses used to calculate the mass-
896 weighted mean of molar masses $<M_w>$. A) Overlay of the elution profiles obtained for TNFα
897 and Ifx, respectively; B1 to B5) Elution profiles for sICs formed after incubation of TNFα and
898 Ifx at different molar ratios.

899

900 **Table S1**

Sample	Range of assigned molar masses [kDa]			Mass-weighted mean of assigned molar masses [kDa]			
	Run 1	Run 2	Run 3	Run 1	Run 2	Run 3	Mean ± SD
Infliximab, IFX	158 – 182	153 – 164	159 – 193	162	156	163	160 ± 4
TNF -alpha	52 – 55	51 – 61	52 – 62	52	52	52	52 ± 0
Immune complexes							
IFX/TNF 3:1	182 – $1.16 \cdot 10^3$	164 – $1.11 \cdot 10^3$	193 – $1.10 \cdot 10^3$	409	398	518	442 ± 66
IFX/TNF 1:1	182 – $2.06 \cdot 10^3$	164 – $1.31 \cdot 10^3$	193 – $1.42 \cdot 10^3$	801	589	681	690 ± 106
IFX/TNF 1:3	182 – $5.05 \cdot 10^3$	164 – $6.89 \cdot 10^3$	193 – $10.8 \cdot 10^3$	$1.77 \cdot 10^3$	$2.00 \cdot 10^3$	$2.61 \cdot 10^3$	$2.13 \cdot 10^3$ ± 435
IFX/TNF 1:9	182 – $5.36 \cdot 10^3$	164 – $3.38 \cdot 10^3$	193 – $3.51 \cdot 10^3$	$1.66 \cdot 10^3$	$1.18 \cdot 10^3$	$1.17 \cdot 10^3$	$1.34 \cdot 10^3$ ± 279
IFX/TNF 1:27	182 – $1.68 \cdot 10^3$	164 – 768	193 – $1.01 \cdot 10^3$	689	464	521	558 ± 117

901

902 **Table S1. Analysis of the molar mass distribution of ICs from AF4 data.**

903 For a given elution time, the AF4 profiles provide the concentration (UV) at which a given
904 molar mass (MALS) of a protein is present in the sample. The molar mass distribution of Ifx,
905 TNFα and their immune complexes (sICs) was obtained by plotting the cumulative frequency
906 as a function of molar mass. For a selected range of molar masses, a mass-weighted mean
907 value ($<M_w>$) was calculated. All detected molar masses were selected in the case of Ifx and
908 TNFα whereas only molar masses larger than the maximal molar mass found for Ifx were
909 assigned to sICs. The table shows the range of assigned molar masses and the calculated
910 $<M_w>$ for each AF4 run (n = 3).